SIMULATION AND OPTIMAL CONTROL OF HYBRID ELECTRIC VEHICLES

Guillermo Becerra[a], Alfonso Pantoja-Vazquez[b], Luis Alvarez-Icaza[c], Idalia Flores[d]

[a],[b],[c] Instituto de Ingenieria-Universidad Nacional Autonoma de Mexico
[d]Posgrado de Ingenieria-Universidad Nacional Autonoma de Mexico
Coyoacan D. F. 04510, Mexico

[a]guillermobec@gmail.com, [b]apantojav@iingen.unam.mx, [c]alvar@pumas.iingen.unam.mx,
[d]idalia@unam.mx

ABSTRACT

New strategies for controlling the power split in hybrid electric vehicles (HEV) are described. The strategies focus in a planetary gear system, where kinematic and dynamic constraints must be fulfillied. The aim is to satisfy driver demands and to reduce fuel consumption. Two strategies are presented, one inspired on optimal control and the other derived from Pontryagin's Minimum Principle. It is shown that, under appropriate choice of weighting parameters in the cost function of the Hamiltonian, both strategies are similar. The resultant power flow control is continuous and uses the internal combustion engine with the maximum efficiency possible. The main advantages are the low computational cost, when compared to other optimization based approaches, and the easiness to tune. The strategy is tested by simulations using a mathematical model of a power train of a hybrid diesel-electric bus subject to the power demands of representative urban area driving cycles. The main elements of the vehicle, internal combustion engine (ICE), battery state of charge (soc), electric machine (EM) and vehicle inertia are simulated with high order models. Simulation results indicate that both strategies achieves small speed tracking errors and attain good fuel consumption reduction levels.

Keywords: Optimal control, Pontryagin's minimum principle, simulation, hybrid electric vehicles, internal combustion engine, electric machine, fuel consumption.

1. INTRODUCTION

Optimal power control on hybrid electric vehicles (HEV) is an important topic for power management. HEV may have different architectures that require the use of diverse energy management strategies. The main architectures, as presented in (John. M. Miller 2006), are series, parallel or series-parallel. A comparison of the architectures is presented in (Ehsani, Gao, and Miller 2007).

Power distribution in HEV can be performed by the use of different controllers, as described in the comparative study of supervisory control strategies for HEV presented in (Pisu and Rizzoni 2007). Rule based approaches can use heuristic, fuzzy logic, neural networks, etc. Examples of these techniques are (Xiong, Zhang, and Yin 2009), that proposes a fuzzy logic control for energy management and (Xiong and Yin 2009), that presents a fuzzy logic controller for energy management of a series-parallel hybrid electric bus with ISG.

There are also power flow control strategies based on optimization, like those revised in (Pisu and Rizzoni 2007). They are normally not implemented in real time, only proved in simulation and their off-line optimization results are used with a look-up table.

(Delprat, Lauber, Guerra, and Rimaux 2004) propose the control of parallel hybrid power train that splits the power between the engine and electric motor in order to minimize the fuel consumption. This strategy optimize the fuel consumption considering the torque engine and the gear ratio.

(Musardo, Rizzoni, and Sataccia 2005) present the Adaptive Equivalent Consumption Minimization Strategy (A-ECMS), which is an algorithm for hybrid electric vehicles that attempts to minimize the vehicle fuel consumption using an equivalence between fuel energy and electric energy. To prove its effectiveness, A-ECMS strategy is compared with Dynamic Programming (DP) and a non adaptive ECMS (Paganelli, Guerra, Delprat, Santin, Delhom, and Combes 2000). (Koot, Kessels, de Jager, Heemels, van den Bosch, and Steinbuch 2005) establish energy management strategies for HEV using dynamic programming and quadratic programming with Model Predictive Control (MPC), to minimize fuel consumption.

(Kim, Cha, and Peng 2011) reported a optimal control of parallel-HEV based on Pontryagin's minimum principle (PMP) that takes into account the state of charge and fuel consumption.They compare the strategy with dynamic programming and ECMS. In (Zou, Teng, Fengchun, and Peng 2013) they compared Pontryagin's minimum principle (PMP) with dynamic programming (DP), finding that the simulation time is significantly lower in PMP than DP. This is important for real time for implementation.

In this paper new strategies to control the power flow in a parallel power train HEV are presented. In this configuration, shown in Fig. 1, the internal combustion engine (ICE) and the electric machine (EM) can directly supply their torque to the driven wheels through a planetary gear

system[1].

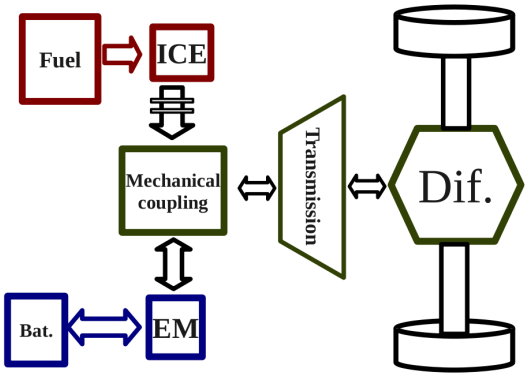

Fig. 1. Parallel hybrid electric vehicle power-train.

The design of the strategies recognizes, as is also pointed out in (Musardo, Rizzoni, and Sataccia 2005), that optimization based solutions to HEV power flow control are very difficult to implement in real-time. Moreover, their results can not be as effective when real driving conditions differ from those used in the optimization problem solution. A similar problem occurs when the uncertainty in the models is considered.

In the first strategy presented this paper, a local criteria is used based on the kinematic and dynamic constrains at the planetary gear system, that must be satisfied when distributing the power demanded by the vehicle between the ICE and EM, and in maximum efficiency curves for the ICE. There are only two pairs of parameters to tune that, as it will be shown later, have a similar behavior for all driving cycles employed in the simulations.

The second strategy is based on PMP and use the errors in the state of charge soc, fuel consumption m_f and power demanded by the user P_d, with respect to some reference values, as system states. Electric power P_{bat} and engine power P_{mci} are system inputs.

To test the developed strategy, simulations of a mathematical model of the main components of the hybrid power-train which includes the ICE and EM, clutch, planetary gear system and battery were performed. The strategy was tested using three standard driving cycles for a bus in Mexico City.

The rest of paper is organized as follows. Section 2 presents the models for simulation of the vehicle subsystems, section 3 describes details the strategies for power flow control. Simulation results are presented in the section 4 while section 5 presents the conclusions and directions for future work.

2. HEV MODELING

2.1. Internal combustion engine model

The model is taken from (Outbib, Dovifaaz, Rachid, and Ouladsine 2002). It is assumed that the air entering the intake manifold follows the ideal gas law and that the manifold temperature varies slowly with respect to pressure and engine speed. The model is described by

$$\begin{aligned} \frac{d\omega_{ice}}{dt} &= \frac{h_1}{\omega_{ice}}\dot{m}_f + h_2 p_a + \frac{h_3}{\omega_{ice}}P_b + \frac{h_4}{\dot{m}_f} \\ \frac{dp_a}{dt} &= h_5\dot{m}_{ai} - h_6\omega_{ice}p_a \end{aligned} \quad (1)$$

and the efficiency is

$$\eta_{ice} = \frac{P_{ice}}{\dot{m}_f p_{th}} \quad (2)$$

where ω_{ice} the engine speed, $\dot{m}_f$ the fuel flow rate used as control signal, p_a the intake manifold pressure, $\dot{m}_{ai}$ air flow entering the manifold, P_b the total brake power, P_{ice} the output power and p_{th} the fuel heating value. Terms h_j are constants determined in the model of (Outbib, Dovifaaz, Rachid, and Ouladsine 2002).

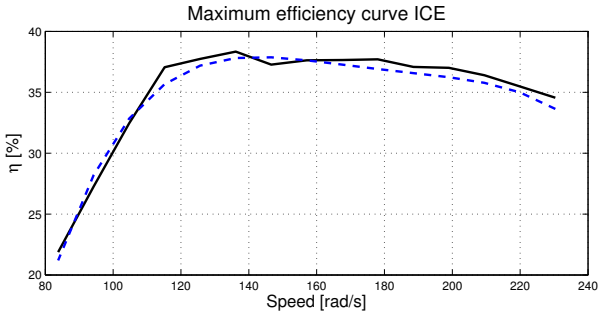

Fig. 2. Efficiency curve of the ICE Diesel

Fig. 2 shown an example of maximum efficiency curve in terms of the engine velocity. One key assumption in Eq. (2) is that air-fuel ratio can be controlled independently of ICE velocity..

2.2. Battery model

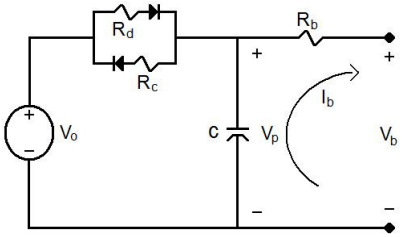

Fig. 3. Battery circuit

In the HEV, batteries are used as a temporary energy storage that helps saving fuel and reducing emissions. The state of charge of the battery (soc) is defined as a measure of the amount of electrical energy stored in it. It is analogous to the fuel gauge in the tank. Its dynamics is given by

$$\dot{soc}(t) = -\frac{P_b}{V_b Q_t} \quad (3)$$

[1]More details about HEV architectures can be found, for example, in (Ehsani, Gao, and Miller 2007)

where $P_b(t)$ is the power, V_b the voltage and Q_t denoting the total charge the battery can store.

The circuit model shown in Fig. 3, contains elements for discharging and charging mode.

2.3. Electrical machine model

The EM is an induction motor that can operate as motor or generator. When operating as motor, it draws power from the battery and the output torque drives the wheels, in possible combination with the ICE torque. Functioning as generator, it can recover kinetic energy from regenerative braking, or take energy from the ICE for battery recharging. Although the model obtained from (Peresada, Tilli, and Tonielli 2004) and used in simulations is fifth order, for the power split strategies it suffices with the relation between output power P_{em} and input power P_{bat} given by

$$P_{em} = \eta_{bm} P_{bat} \tag{4}$$

where η_{bm} is battery and EM efficiency.

2.4. Planetary gear system

The coupling of the power sources to traction is accomplished through a planetary gear system (PGS). Fig. 4 shows a schematic of this mechanical device. The ICE is connected through a clutch-brake to the sun gear of the PGS, the EM is connected to the ring gear and the wheels are connected to the carrier gear (Ambarisha and Parcker 2007),(Szumanowski, Yuhua, and Pi´orkowski 2005).

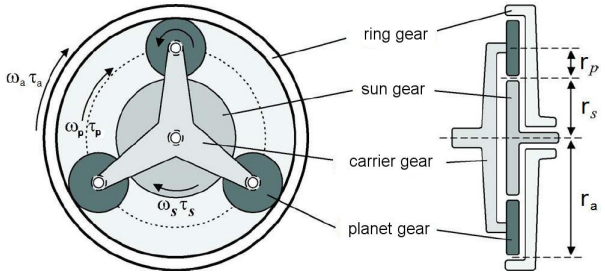

Fig. 4. Planetary gear system

The gear ratio is $k = \frac{r_a}{r_s}$, where r_a is the ring gear radius, r_s the sun gear radius and the angular velocities in the PGS satisfy

$$\omega_p = \frac{1}{(k+1)}\omega_s + \frac{k}{(k+1)}\omega_a \tag{5}$$

where ω_p, ω_s and ω_a are the angular velocities of the planet carrier, ICE and EM.

The balance of power in the PGS satisfies

$$P_p = T_s\omega_s + T_a\omega_a \tag{6}$$

Eqs. (5)-(6) are the kinematic and dynamic constraints, respectively, that any power flow strategy that employs a PGS must satisfy at all times.

The PGS is equipped with appropriate brakes to allow only one power source when convenient.

2.5. Clutch system

To disengage the ICE from the sun gear of the PGS a clutch is included (see Fig. 5). Three modes of operation

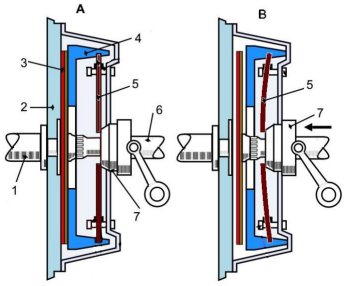

Fig. 5. Clutch system.

for the clutch are modeled: when the ICE is disengaged, sliding and engaged (James and Narasimhamurthi 2005).

The clutch is modeled by

$$(J_{ice} + J_{clu})\dot{\omega}_{ice} = T_{ice} - T_{clu} - T_f \tag{7}$$

where J is the inertia, ω the velocity, T the torque, subscripts ice, clu and f are for ICE, clutch and friction, respectively. When the clutch is disengaged, $T_{clu} = 0$. When it is slipping,

$$\begin{aligned} T_{clu} = &\left[k_{e1}\int(\mid \omega_{ice} - \omega_{clu} \mid)dt\right] \times \\ &[\mid (\omega_{ice} - \omega_{clu}) \mid (-0.0005) + 1] \times \\ &f(\mid \omega_{ice} - \omega_{clu} \mid) \end{aligned} \tag{8}$$

where, k_{e1} is the stiffness coefficient of sliding.

Finally, when the clutch is engaged $\omega_{ice} = \omega_{clu}$ and

$$\begin{aligned} T_{clu} = &k_{e2}(\int(\omega_{ice} - \omega_{clu})dt) + \\ &f_{es}(\omega_{ice} - \omega_{clu}) \end{aligned} \tag{9}$$

where k_{e2} is a stiffness coefficient, f_{es} an absorption coefficient.

2.6. Vehicle model

Vehicle is modeled like a moving mass subjected to a traction force $F_{tr}(t)$. The forces at the power-train also include the aerodynamic drag force $F_a(t)$, the rolling resistance $F_r(t)$ of the tires and the gravitational force $F_g(t)$ induced by the slope in the road, that are given by (Xiong, Zhang, and Yin 2009), (Kessels, Koot, van den Bosch, and Kok 2008)

$$\begin{aligned} F_a(t) &= 0.5\rho_a v(t)^2 C_d A_d \\ F_r(t) &= mgC_r \cos\gamma(t) \\ F_g(t) &= mg\sin\gamma(t) \end{aligned} \tag{10}$$

where ρ_a is the air density, $v(t)$ the vehicle speed, C_d the aerodynamic drag coefficient, A_d the vehicle frontal area, m the vehicle mass, g the gravity acceleration constant, C_r the tire rolling resistance coefficient and γ the road slope.

The vehicle velocity $v(t)$ dynamics is given by

$$m\frac{dv(t)}{dt} = F_{tr} - F_a(t) - F_r(t) - F_g(t) \tag{11}$$

3. POWER FLOW CONTROL STRATEGIES

It is assumed that the ICE and EM are controlled with two independent controllers, whose set points must be determined by power flow control strategy.

The approach developed in this paper is based in the following observations:

1) The most important requirement in HEV power flow control is the ability to satisfy driver requirements.
2) All optimal solutions to power flow control preserve the state of charge of batteries, averaged over a long enough time period.
3) To minimize fuel consumption, ICE must be operated at high efficiency regions.

Observation 2, key in this paper strategy, is easily confirmed by noticing that all optimal solutions based on driving cycles must preserve the initial state of charge on the batteries at the end of cycle, otherwise the vehicle can not sustain repetitions of the same cycle. A similar observation is also made in Musardo et al (Musardo, Rizzoni, and Sataccia 2005), when discussing the tuning of A-ECMS. Observation 3 can be verified, for example, in (John. M. Miller 2006) or (Ehsani, Gao, and Miller 2007), and it is one of the main reasons HEV are overall more efficient that normal vehicles.

3.1. Optimal strategy

This strategy is based on PMP. The problem is to find an admissible control $u^* \in U$ that causes the system

$$\dot{x}(t) = a(x(t), u(t), t) \tag{12}$$

to follow an admissible trajectory $x^* \in X$that minimizes the performance cost

$$J(u) = h(x(t_f), t_f) + \int_{t_0}^{t_f} g(x(t), u(t), t)dt \tag{13}$$

Using as system state the errors in the demanded power $e_{P_p} = P_p - P_d$, state of charge $e_{soc} = soc - soc_{ref}$ and fuel flow $e_{m_f} = m_f - m_{f_{ref}}$, and the battery power and engine power $u^T = [P_{bat} \quad P_{ice}]$ as inputs. It follows that

$$\begin{aligned} e_{P_p} &= \eta_{me}P_{bat} + P_{ice} - P_d \\ \dot{e}_{soc} &= -\frac{1}{V_{bat}Q_{nom}}P_{bat} - s\dot{o}c_{ref} \\ \dot{e}_{m_f} &= \frac{P_{ice}}{\eta_{ice}p_{th}} - \dot{m}_{f_{ref}} \end{aligned} \tag{14}$$

where P_d is the demanded power and P_p the power supplied by the engines.

The performance cost can be expressed as

$$\min J = \int e^T G_1 e + u^T G_2 u \quad dt \tag{15}$$

where G_1 and G_2 are appropriate weighting matrices.

The Hamiltonian is defined as

$$H = e^T G_1 e + u^T G_2 u + p^T[a(e, u, t)] \tag{16}$$

Using this notation, the necessary conditions to find the optimal control $u^* \in U$ that causes an admissible trajectory $e^* \in X$ and minimizes the performance cost as follows:

$$\begin{aligned} e_{P_p} &= \eta_{me}u_1 + u_2 - P_d \\ \dot{e}_{soc} &= -\frac{1}{V_{bat}Q_{nom}}u_1 \\ \dot{e}_{m_f} &= \frac{u_2}{\eta_{mci}p_{th}} \end{aligned} \tag{17}$$

where the soc and m_f are assumed constant references with zero time derivatives.

The costate equations are

$$\begin{aligned} \dot{p}_1 &= g_{11}e_{P_p} \\ \dot{p}_2 &= g_{12}e_{soc} \\ \dot{p}_3 &= g_{13}e_{m_f} \end{aligned} \tag{18}$$

and the restriction for the inputs are as follows

$$\begin{aligned} 0 &= g_{21}u_1^* + p_1\eta_{me} - p_2\frac{1}{V_{bat}Q_{nom}} \\ 0 &= g_{22}u_2^* + p_1 + p_3\frac{1}{\eta_{mci}p_{th}} \end{aligned} \tag{19}$$

If Eq. (19) is solved for u^* and substituted into the state Eqs. (17), three equations for the state and three for the costates are obtained

$$\begin{aligned} e_1^* &= \eta_{me}u_1^*(p_1, p_2) + u_2^*(p_1, p_3) - P_d \\ \dot{e}_2^* &= -\frac{1}{V_{bat}Q_{nom}}u_1^*(p_1, p_2) \\ \dot{e}_3^* &= \frac{1}{\eta_{mci}p_{th}}u_2^*(p_1, p_3) \\ \dot{p}_1^* &= g_{11}e_1^* \\ \dot{p}_2^* &= g_{12}e_2^* \\ \dot{p}_3^* &= g_{13}e_3^* \end{aligned} \tag{20}$$

Eqs. (20), the state and costate equations, are a set of linear first order, homogeneous algebraic-differential equations, that distribute power optimally between EM and ICE, given parameters G_i.

3.2. PGS Strategy

The second strategy, named PGS strategy, is inspired in optimal control and tries to reduce fuel consumption by using the EM as much as possible, that is, by maximizing electrical energy use. Assuming that the state of charge in the batteries must be kept at a reference value, for the traction case, $P_p > 0$,

$$J_1 = max(\int_0^{T_c} (sign(P_p)sign(soc - soc_{ref}))P_{me}dt \tag{21}$$

where T_c is the duration of the driving cycle, soc_{ref} is a reference value for soc. This expression is useful for the cases of traction and traction-recharging batteries.

For the braking case, $P_p < 0$, the criteria is

$$J_2 = \max \int_0^{T_c} (sign(P_p)P_{em})\ dt \tag{22}$$

The value of Eqs. (21)-(22) is maximized when $P_{me} = \min\{sign(P_p)P_p, sign(P_p)P_{em}^{max}\}$, with P_{em}^{max} the maximum power attainable by the EM (assumed equal for the motor and generator cases). To avoid the switching induced by $sign(P_p)$ a smooth function of the soc is used. Therefore

$$P_{em} = P_{em}(soc) = \alpha_i(soc)P_{em}^{max} \quad (23)$$

where subindex in Eq. (23) is 1 when $P_p > 0$ and 2 when $P_p < 0$, $\alpha_i \in [-1, 1]$.

Assuming that P_p and ω_p are known, the proposed solution to the power flow control starts by substituting Eq. (23) in Eq. (6) leads to

$$P_p = \alpha_i P_{em}^{max} + P_{ice} \quad (24)$$

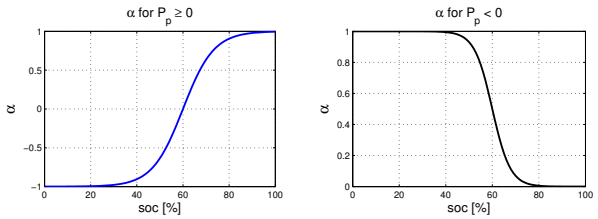

Fig. 6. α for $P_p \geq 0$ and $P_p < 0$

The shape of $\alpha_i(soc)$ determines how much electric power is taken or delivered at a given point. One possible choice for $\alpha_i(soc)$ is shown in Fig. 6, that is described by

$$\alpha_1 = \tanh(A_1(soc - soc_{ref})) \qquad Pp \geq 0 \quad (25)$$

$$\alpha_2 = 0.5 - 0.5(\tanh(A_2(soc - soc_{full}))) \qquad Pp < 0 \quad (26)$$

where soc_{ref} is a reference value for the batteries if the EM acts as a motor and soc_{full} is a reference value to avoid battery overcharging in the generator case.

If α_1 is positive the EM operates as motor, otherwise it operates as generator. Fig. 6 reveals that when $P_p \geq 0$, $\alpha_1 \in [-1, 1]$ depending on the state charge of the battery. When $P_p < 0$, $\alpha_2 \in [0, 1]$, regenerative braking is possible and the EM can work only as generator. This choice allows to make maximum use of electric power for traction or recharging of the batteries.

With α_i chosen, electric power in Ec.(24) is fixed. P_{ice} is determined as follows:

$$P_{ice} = min(P_p - P_{em}, P_{ice}^{max}); \quad P_p \geq 0$$

that guarantees that the ICE provides power below its maximum available power P_{ice}^{max}.

3.3. Assigning speed and torque

Given P_{ice}, the angular velocity at which the ICE must operate, ω_{ice}, is obtained from the maximum efficiency curve in the power vs. angular velocity curve. This curve has a shape similar to that shown in Fig. 7 and is approximated by a polynomial with P_{ice} as independent variable. With this choice, it is assured that the ICE is always used with maximum efficiency.

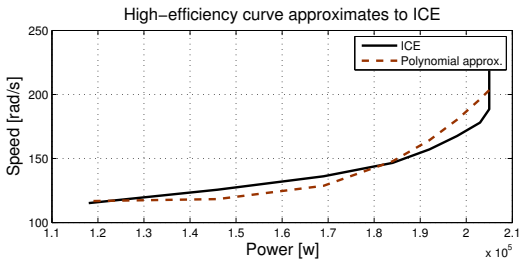

Fig. 7. Power vs. Speed high efficiency curve of the ICE.

Once ω_{ice} is obtained from the maximum efficiency curve, the required torque is

$$T_{mci} = \frac{P_{mci}}{\omega_{mci}} \qquad for \qquad \omega > 0 \quad (27)$$

$$T_{mci} = 0 \qquad for \qquad \omega = 0 \quad (28)$$

The final step is to determine the angular velocity and torque for the EM. From Eq. (5) ω_{em} is

$$\omega_{me} = \frac{(k+1)}{k}(\omega_p - \frac{1}{(k+1)}\omega_{mci}) \quad (29)$$

and the torque T_{em} is derived from

$$T_{me} = \frac{P_{me}}{\omega_{me}} \qquad for \qquad \omega > 0 \quad (30)$$

$$T_{me} = 0 \qquad for \qquad \omega = 0 \quad (31)$$

4. SIMULATION RESULTS

Simulations were carried out on SIMULINK MATLAB software for a bus with mass of 15,000 $[kg]$, a diesel ICE of 205 $[kw]$, a clutch between the ICE and a PGS with $k = 5$. The electric machine is a induction motor of 93 $[kw]$ and the batteries are $25[Ah]$ at $288[V]$. ll the components were simulated and tested separately. The bus is commanded to follow the three standard driving cycles: low velocity (1) c_1, medium velocity (2) c_2 and high velocity (3) c_3. On example of a driving cycle is shown in Fig. 8.

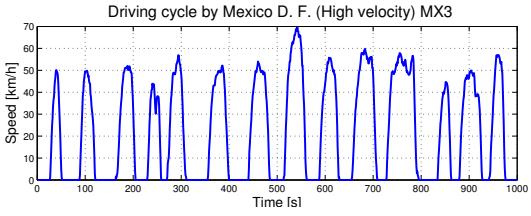

Fig. 8. High velocity driving cycle, c3

As mentioned before, the most important feature of any power flow control strategy in HEV is the ability to track driver power demands. Typical examples of speed tracking capability are shown in Fig. 9, that illustrate, for driving cycles 2 and 3, the velocity of the HEV obtained by the PMP strategy and velocity obtained by the PGS strategy. Velocity tracking is very good for both strategies. The first observation that inspired the strategies is satisfied.

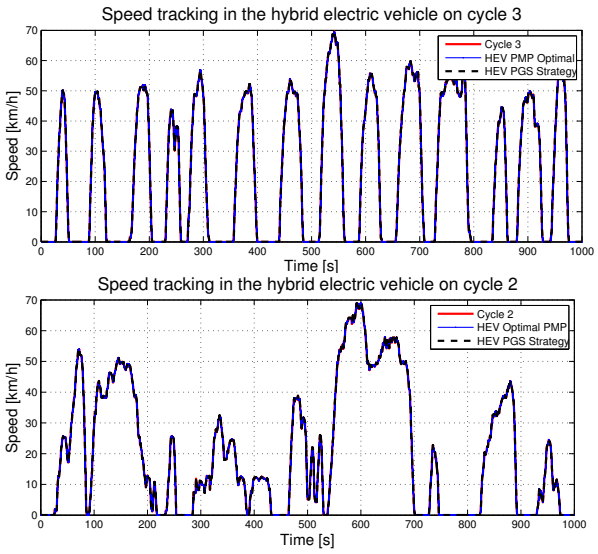

Fig. 9. HEV velocity tracking, high and medium velocity

Fig. 10 and Fig. 11 show simulation results of the state of charge (soc) for PMP strategy (blue dashed line) and PGS strategy (red continuous line). Note that the oscillations are bigger for the PMP strategy and that both strategies have the same initial and final state of charge.

If the soc initial an final is same for both strategies, the fuel consumption is considered net spending for the comparative index and the vehicle can be repeated the driving cycle as many times as required.

If the battery pack is more small, the oscillations are bigger for the dynamic soc.

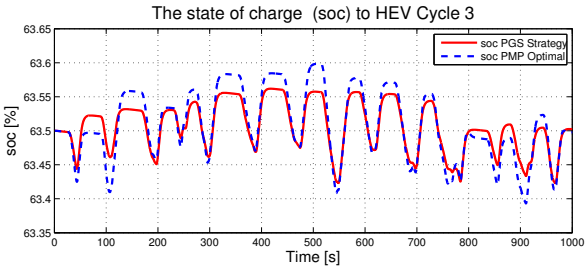

Fig. 10. soc for PGS strategy and PMP strategy, cycle c3

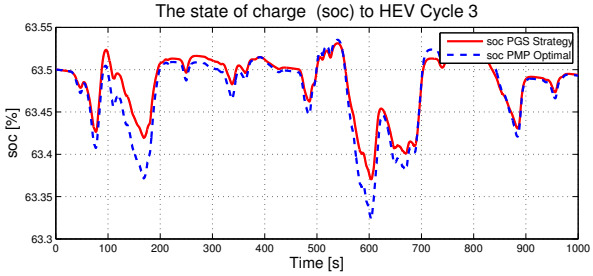

Fig. 11. soc for PGS strategy and PMP strategy, cycle c2

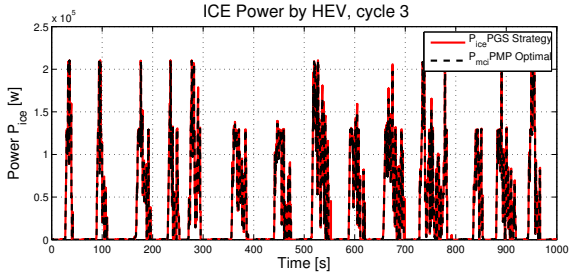

Fig. 12. ICE power compared for PGS and PMP strategies, cycle c3

The resultant ICE power is shown in Fig. 12 and the EM power Fig. 13 for the high velocity driving cycle (MX3), (black dashed line) for PMP strategy and (red continuous line) for the PGS strategy. Power requirements are very similar.

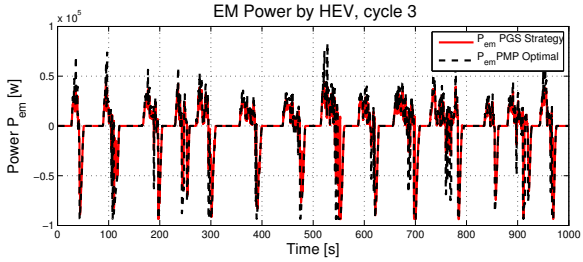

Fig. 13. EM power compared for PGS and PMP strategies, cycle c3

To convey an idea of the fuel consumption reduction provided by the HEV power split strategies, table I compares the total fuel consumption for two driving cycles and for a vehicle equipped only with an ICE. Notice the small difference between the fuel consumption of the two presented strategies.

Table I
COMPARISON OF STRATEGIES

Strategy	Cycle	Consumption (kg)	Consumption (%)
Only ICE	3	17.36	100
PMP	3	10.36	59.68
PGS	3	10.5	60.48
Only ICE	2	10.13	100
PMPl	2	7.976	78.74
PGS	2	8.029	79.26

5. CONCLUSIONS

A pair of power split strategies for HEV were presented and proved by simulations on SIMULINK-MATLAB software. The strategy is designed for a parallel configuration HEV where a planetary gear system is used a power coupling device. Simulations use a detailed model of a HEV that includes a diesel internal combustion engine, an induction electric engine, a planetary gear system, a clutch, batteries and gear transmission.

The first strategy is based on Pontryagin's minimum principle (PMP), while the second is designed around

a planetary gear system (PGS). Design procedures are described to obtain power and torque splits. Simulation were performed in such a way that initial and final state of charge of batteries is equal for all driving cycles. Results show that, by appropriate tuning of the weighting matrices in the Hamiltonian of the PMP strategy, both strategies achieve very similar results. However, the information requirements and the computational cost of the PGS strategy are smaller than those of the PMP strategy, making the first strategy more suitable for real time implementation.

Results also indicate excellent tracking of all driving cycles with limited excursions of the battery state of charge during the driving cycle. ICE operates at high efficiency, given the power split determined by both strategies.

An adaptive version and experimental testing of the strategies is ongoing work.

6. ACKNOWLEDGMENT

This research was supported by CONACYT grant 103640, UNAM-PAPIIT grant IN105512 and UNAM-PAPIIT grant IN116012. The first two authors specially acknowledge the support from CONACYT scholarship program.

REFERENCES

Ambarisha, V. K. and R. G. Parcker (2007, January). Nonlinear dynamics of planetary gears using anlytical and finite element models. *Journal of sound and vibration 302*, 577–595.

Delprat, S., J. Lauber, T. M. Guerra, and J. Rimaux (2004, May). Control of a Parallel Hybrid Powertrain: Optimal Control. *IEEE Transactions on Vehicular Technology 53*, 872–881.

Ehsani, M., Y. Gao, and J. M. Miller (2007, April). Hybrid Electric Vehicles: Architecture and Motor Drives. *Proceedins of the IEEE 95*, 719–728.

James, D. and N. Narasimhamurthi (2005, 8-10, June). Design of a optimal controller for commercial trucks. In *American Control Conference*, Portland, Oregon, USA., pp. 1599–1606.

John. M. Miller (2006, May). Hybrid Electric Vehicle Propulsion System Architectures of the e-CVT Type. *IEEE Transactions on Power Electronics 21*, 756–767.

Kessels, J. T. B. A., W. T. Koot, P. P. J. van den Bosch, and D. B. Kok (2008, november). Online Energy Management for Hybrid Electric Vehicles. *IEEE Transactions on Vehicular Technology 57*, 3428–3440.

Kim, N., S. Cha, and H. Peng (2011, September). Optimal control of hybrid electric vehicles based on pontryagin's principle. *IEEE Transactions on Control Systems Technology 19*, 1279–1287.

Koot, M., J. T. B. A. Kessels, B. de Jager, W. P. M. H. Heemels, P. P. J. van den Bosch, and M. Steinbuch (2005, May). Energy Management Strategies for Vehicular Electric Power Systems. *IEEE Transactions on Vehicular Technology 54*, 771–782.

Musardo, C., G. Rizzoni, and B. Sataccia (2005, December). A-ECMS: An Adaptive Algoritm for Hybrid Electric Vehicle Energy Management. In *44th IEEE Conference on Decicsion and Control, and the European Control Conference*, Seville, Spain., pp. 1816–1823.

Outbib, R., X. Dovifaaz, A. Rachid, and M. Ouladsine (2002, May). Speed control of a diesel engine: a nonlinear approach. In *American Control Conference*, Anchorage, Alaska, USA., pp. 3293–3294.

Paganelli, G., T. M. Guerra, S. Delprat, J.-J. Santin, M. Delhom, and E. Combes (2000). Simulation and assessment of power control strategies for a parallel hybrid car. *Journal of automobile engineering 214*, 705–717.

Peresada, S., A. Tilli, and A. Tonielli (2004). Power control of a doubly fed induction machine via output feedback. *Control Engineering Practice 12*, 41–57.

Pisu, P. and G. Rizzoni (2007, may). A Comparative Study Of Supervisory Control Strategies for Hybrid Electric Vehicles. *IEEE Transactions on Control Systems Technology 15*, 506–518.

Szumanowski, A., C. Yuhua, and P. Piórkowski (2005, sept). Analysis of Different Control Strategies and Operating Modes of Compact Hybrid Planetary Transmission Drive. *Vehicle Power and Propulsion 7*, 673–680.

Xiong, W., Y. Zhang, and C. Yin (2009, July). Optimal Energy Management for a Series-Parallel Hybrid Electric Bus. *Energy conversion and management 50*, 1730–1738.

Xiong, W. W. and C. L. Yin (2009, May). Design of Series-parallel Hybrid Electric Propulsion Systems and Application in City Transit Bus. *WSEAS Transaction on Systems 8*, 578–590.

Zou, Y., L. Teng, S. Fengchun, and H. Peng (2013, April). Comparative study of dynamic programming and pontryagin's minimum principle on energy management for a parallel hybrid electric vehicle. *Energies 6*, 2305–2318.

AUTHORS BIOGRAPHY

Guillermo Becerra Was born in Colima, Mexico in 1986. B. S. degree in Mechanical and Electrical Engineering from the Universidad de Colima, Mexico in 2008, the M. S. degree in Electrical Engineering from the Universidad Nacional Autónoma de México UNAM, Mexico in 2010 and he is currently a Ph. D. candidate in (Control) Electrical Engineering at the UNAM, Mexico and since 2011 he joined the Department of Mechatronics Engineering, UNAM, as an Interim Professor. His research interests include nonlinear control theory, mechatronics, optimal control and applications.

Alfonso Pantoja-Vazquez Recived the B. S. degree in instrumentation and process control engineering from the University of Queretaro, Mexico in 2003, the M. S. degree in electrical engineering from the Universidad Nacional Autónoma de México, Mexico in 2006 and he is currently a Ph. D. candidate in Mechatronics Engineering at the Universidad Nacional Autónoma de México, Mexico. He worked for Delphi from 2007 to 2011 as embedded software engineer for automotive devices. He joined the University of Quererraro from 2010 to 2011 as interim professor on the embedded software department and since 2011 he joined the department of mechatronics engineering at the Natinoal University of Mexico, as interim professor. His research interests include mechatronics, embedded software, optimal control and its applications.

Luis Alvarez-Icaza Was born in México City. Obtained his PhD in Mechanical Engineering at University of California in Berkeley. He is Professor at Instituto de Ingeniería of the Universidad Nacional Autónoma de México. He is currently Dean of Graduate Studies of Engineering. His research interests are in the areas of vehicle control, buildings vibration control, wind generators control and traffic control.

Idalia Flores She received her Ph.D. in Operations Research at the Faculty of Engineering of the UNAM. She graduated Master with honors and received the Gabino Barreda Medal for the best average of her generation. She has been a referee and a member of various Academic Committees at CONACYT. She has been a referee for journals such as Journal of Applied Research and Technology, the Center of Applied Sciences and Technological Development, UNAM and the Transactions of the Society for Modeling and Simulation International. Her research interests are in simulation and optimization of production and service systems. She is a full time professor at the Postgraduate Program at UNAM.